



## Laser activated single-use micropumps



G.P. Kanakaris, N. Fatsis-Kavalopoulos, L.G. Alexopoulos\*

National Technical University of Athens, Mechanical Engineering, Iroon Polytechniou Str. 9, 15780 Athens, Greece

### ARTICLE INFO

#### Article history:

Received 29 January 2015  
Received in revised form 3 April 2015  
Accepted 22 April 2015  
Available online 12 June 2015

#### Keywords:

Microfluidic liquid handling  
Expandable microspheres  
Micropumps  
Optofluidics  
Lab on a Chip

### ABSTRACT

Lab on Chip technologies have enabled the possibility of novel  $\mu$ TAS devices (micro Total Analysis System) that could drastically improve health care services for billions of people around the world. However, serious drawbacks that reside in fluid handling technology currently available for these systems often restrict the commercialization of such devices. This work demonstrates a novel fluid handling method as a possible alternative to current micropumping techniques for disposable microfluidic chips. This technology is based on a single use, low cost, thermal micropumping system in which expandable microsphere mixtures are activated by commercial grade laser diodes to achieve flow rates as high as 2.2  $\mu$ l/s and total volumes over 160  $\mu$ l. With the addition of a volume dependent shut off valve, nanoliter repeatability is realized. Pressure and heat transfer related data are presented. Finally, the possible prospects and limitations of this technology as a core element in unified optofluidic systems are discussed.

© 2015 The Authors. Published by Elsevier B.V. This is an open access article under the CC BY-NC-ND license (<http://creativecommons.org/licenses/by-nc-nd/4.0/>).

### 1. Introduction

Microfluidic systems have grown to become a very important factor in the design of  $\mu$ TAS, especially when the goal is the design for manufacturability (DFM) or the design for usability of a system.  $\mu$ TA Systems add portability and accessibility in a large variety of protein analysis, genomic analysis, disease diagnostics, disease monitoring, environmental analysis and other procedures, while at the same time have the potential to reduce costs and increase assay sensitivity. However, from a plethora of proposed  $\mu$ TAS technologies, few are finally realized in commercial systems since they are often hard to implement within the boundaries of industrial and commercial favorability.

Among many design considerations that need to be addressed, fluid handling inside a microfluidic system has proven to be quite challenging. As far as pumping is concerned, off-the-shelf components such as piston and peristaltic pumps suffer among other things from chip connectivity, cost, usability, modularity, dead volume and maintenance issues. For this reason, on-chip integration of fluid handling components has gained popularity over the last few years as an alternative to peripheral support equipment.

Several systems and methods for the partial or complete integration of active micropumps in microfluidic systems has been proposed, based on a variety of principles and technologies [1]. The revolutionary Quake valve technology, based on pneumatic

actuation, has been used to fabricate embedded micropumps [2]. Peristaltic action has also been used with normally open [3] or normally closed [4] architecture for rectangular profile channels, while single stroke systems have been developed [5,6] in an effort to reduce the number of actuators per micropump. Piezoelectric elements [7,8] and Braille pins [9] have been used as actuators in the same manner. Other technologies include electrochemical processes [10], electroosmotic flow pumping systems [11], acoustic systems [12], magnetohydrodynamic micropumps [13], electrowetting [14], PDMS gas permeation systems [15], Optically driven thermoviscous expansion [16], opto-electrical-thermal transduction [17] and, of particular interest to this work, thermal micropumping that utilizes expandable microspheres embedded in a PDMS matrix [18–20]. While all of these methods have been successfully applied in laboratory environment, one common limitation is the inherent requirement of bulky and/or costly peripheral devices to support microfluidic functions. In other cases, integrated components often require complex manufacturing procedures that increase cost, or complex structures that introduce additional failure modes in the microfluidic operation.

This work presents a simple, fully integrated, on-chip liquid handling method in which a mixture consisting of expandable microspheres, an absorbance agent and a carrier liquid expand when heated by an infrared laser beam. Flow and pressure characteristics of the proposed micropumping method are evaluated as a function of the mixture composition. We introduce the placement of an ultraviolet laser diode which enables volume displacement control by inducing a photochemical process in a UV curing material. Finally, the pros and cons of this proposed method are

\* Corresponding author. Tel.: +30 210 7721516.  
E-mail address: [leo@mail.ntua.gr](mailto:leo@mail.ntua.gr) (L.G. Alexopoulos).

discussed, as well as the potential that arises from this technology toward the development of reliable, low cost  $\mu$ TA optofluidic platforms for in vitro diagnostics.

## 2. Materials and methods

### 2.1. Preparation of laser activated expandable mixtures

Expancel<sup>®</sup> microspheres (AkzoNobel NV, Amsterdam, Netherlands) are microscale particles of 5–9  $\mu$ m diameter. They consist of a thermoplastic shell which encapsulates a pressurized hydrocarbon in liquid state. Above a specific temperature, the shell becomes pliable allowing the expansion of the particle due to its initial internal pressure and additional pressure due to heat input. Up to that point, the microsphere will not contract substantially if cooled. If additional heat is introduced in the environment of the microsphere, the particles will display some shrinkage upon a consequent cooling of the area. Upon further heating, the shell ruptures and the gas is released. Since microspheres themselves present low absorbance in the near-IR spectrum, we designed a carrier that introduces high IR absorbance and acts as a sealant for the released hydrocarbon from the ruptured beads, thus preventing the gas from leaking into the microfluidic chambers. We tested various compositions of Expancel<sup>®</sup> DU 40 particles, dimethicone silicone oil and carbon black particles mixed into a viscous composition. DU 40 particles start expanding at 80 °C, the lowest activating temperature for available expandable microspheres. Silicon oil was chosen because of its inert, non-toxic nature, its optical properties and its availability. Carbon black was chosen because of its wide absorbance spectrum, its availability and cost. Overall, the mixture was designed for cost and for compliance with industry-friendly chip designs such as imprinted or molded polymer structures.

### 2.2. Chip fabrication and verification

Microfluidic chip structures (channels and chambers), were fabricated using either a commercial grade laser engraver (initial experiments) or a standard 3 axis CNC milling machine for improved dimensional repeatability. The chip stocks were commercial grade PMMA 1 × 3 in. 2 mm thick slides. After fabrication, chips were washed in an ultrasonic bath and their pattern depth was measured in a microscope using a 40× objective lens of 1  $\mu$ m depth of field and a precision micrometer (1  $\mu$ m resolution). A number of chips of varying depths were connected to a LabSmith<sup>®</sup> positive displacement microfluidic pump (LabSmith Inc, Livermore, CA) in order to find the correlation of the chip's volume capacity and the structure depth by incrementally pumping 1 to 0.05  $\mu$ l inside the microfluidic meander until it was full. The laser engraved structures had a depth of  $364 \pm 8.33 \mu\text{m}$  (1 standard error). The microfluidic channel profile and cross section, with a nominal width of 500  $\mu$ m, were measured in a sample of chips to obtain a mean of variation coefficients equal to 5.5% in cross sectional area of each individual chip using a Matlab<sup>®</sup> pixel count algorithm and a calibration microscope slide. The machined structures had a mean depth of  $511 \pm 3.2 \mu\text{m}$  and channel width equal to 1000  $\mu$ m in a semi-circular profile. The chips were sealed with microscope slides or glass coverslips and optically clear UV adhesive where optical clarity or heat resistance was of the essence. Thick transparent adhesive membrane was used for less demanding chip positions. All reagents were injected manually into their respective positions using 500  $\mu$ l syringes and 30 G hypodermic needles. The orifices created by the needles on the sealant were shut using UV curing photopolymer plugs.

### 2.3. Experimental setup

Microfluidic chips were placed between a laser source and a CCD camera. Laser sources used were continuous wave commercial grade diode lasers. The sources used for activation were 980 nm diodes of 531 mW laser power, 15.2% unit efficiency and 87 mW/mm<sup>2</sup> power density at an approximate 1.4 mm spot size at entry point. The sources used for displacement control (photopolymerization lasers) were 405 nm diodes of 62 mW laser power, 25.5% unit efficiency and 78 mW/mm<sup>2</sup> power density. Focusing was achieved using a collimator and a focus lens which were manually adjusted. A CCD camera placed on top of the microfluidic chips recorded all experiments to obtain relevant data with video analysis tools. Pressurizing of the chip outlet was achieved using an Elveflow<sup>®</sup> pressure generator (ELVESYS, Pépinière Paris Santé Cochin). The liquid reagent substitutes are red and blue water-soluble dyes. For the Set Volume Displacement experiments, the photopolymer used was a standard medical device UV adhesive by Loctite<sup>®</sup> (Henkel AG & Company, KGaA, Düsseldorf, Germany) with relatively low viscosity (300 cP) and fast curing time (ISO 4587, Fusion<sup>®</sup> D light source, 50 mW/cm<sup>2</sup>, CT <5 s). In heat flow experiments, images were acquired using a FLIR<sup>®</sup> T335 thermal imaging camera (FLIR GmbH, Frankfurt, Germany).

### 2.4. Video analysis tools

Custom video analysis tools were developed in Matlab<sup>®</sup>. The algorithm identifies predetermined nodes along microfluidic channels that are tracked based on their color value in order to obtain displaced volume against time diagrams. In repeatability experiments, the algorithm tracks the displaced volume continuously by overlapping a virtual fluid path on the microfluidic channel and quantifying color and intensity values versus time. As post processing steps, the tool uses as a secondary input the specifics of each experiment, such as channel depth and trigger times of laser diodes, to provide with accurate diagrams on flow, volume displacement and segmentation of volume displacement into linear and nonlinear regions.

## 3. Results

### 3.1. Single use micropump design

The principle of operation for the developed micropump is shown in Fig. 1. The mixture is placed in a chamber at one end of a microfluidic system enclosed laterally by optical windows that facilitate the entry of an infrared laser beam. The microfluidic system consists of two chambers, one filled with the microsphere mixture and one empty in line with a liquid filled chamber (Fig. 1A). The empty chamber's purpose is to accommodate microsphere mixture being displaced due to the expansion. Upon activation of the laser diode (Fig. 1B) heat is added locally to the entry point of the beam and the first layer microspheres expand in volume thus pushing the unexpanded mixture into the empty cavity and the liquid reagent (aqueous dye solution) in line the microfluidic path. Subsequently, as temperature continues to rise locally, internal pressure builds up in the microspheres which eventually burst. The released hydrocarbon remains enclosed by the rest of the mixture (Fig. 1C) creating a bubble transmissive to the infrared beam.

This process allows for the laser beam to proceed through the mixture layer by layer and maximize expansion by only locally heating a percentage of the mixture at every given time. Until the peak of the beam profile reaches the upper level of the microsphere chamber, the expansion is linear, since the same amount of beads is available for activation at each layer. Once the beam starts exiting

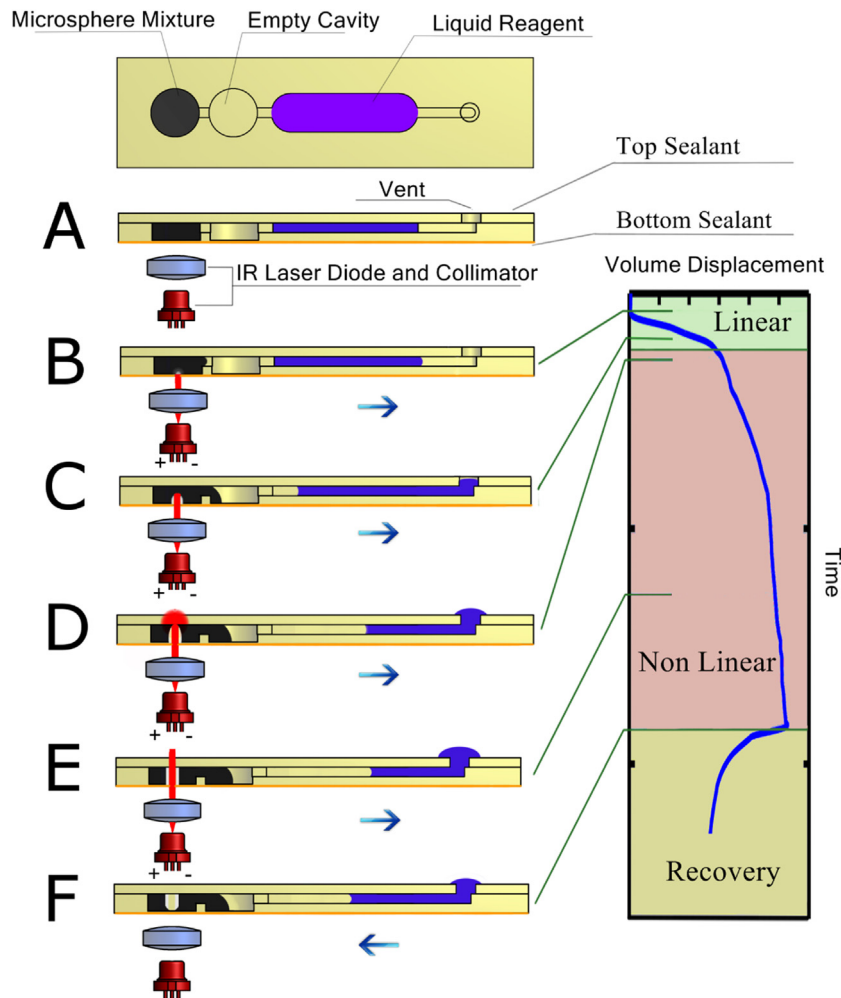


**Fig. 1.** Top and cross sectional views of the example microfluidic chip undergoing a mixture activation process. Initially the laser source is deactivated (A). Upon laser activation (B) we observe linear volume displacement in respect to time (C). In sections (D, E) nonlinear expansion takes place. (F) represents the deactivation of the laser after which there is partial retraction of the displaced volume.

the chamber, the volume displacement rate drops (Fig. 1D). When the beam has fully penetrated the mixture (Fig. 1E) a region around the created orifice continues to be excited by a lower power portion of the Gaussian profile laser beam. Some heat is still added to the mixture, but the expansion continues at a very low rate. Once the diode is deactivated, the heat input stops, causing a reduction of internal pressure, and part of the displaced mixture volume returns to the initial liquid containing chamber (Fig. 1F). In order to characterize the proposed technology, we examined the key parameters of this method: flow rate and volume displacement, displaced volume repeatability (utilizing additional methods), pressure build-up capability and heat transfer from the pump to the reagents.

### 3.2. Volume displacement and flow rate experiments

In order to examine how the volume displacement and flow rate depend on the mixture composition, we performed experiments of mixture activation inside a microfluidic chip embodying a calibrated meander channel for volume tracking (Fig. 2A) in line with the mixture and reagent chambers described in Section 3.1. Upon activation of the laser diode, the camera would start recording the volume displacement, during which the laser beam would cause the mixture to expand and act as a micropump for the liquid solution, pushing it into the meander channels.

Various experiments were conducted in order to assess the effect of the expandable mixture composition. Four compositions

were tested under the same conditions, starting from a less concentrated mixture of 5 g of microspheres and 0.25 g of carbon black in 30 g silicon oil medium, up to quadruplet quantities of the active ingredients in the same amount of medium. What can be observed in Fig. 2B is the presence of a linear and a non-linear curve segment in the expansion process, which was discussed in Section 3.1. Specific data are shown in Table 1. Each experiment was conducted in five replicates. We define as Linear, the part of the curve for which a linear regression model can be applied with a coefficient of determination  $R^2 \geq 0.99$ . We define as “Linear flow rate” the flow rate acquired from the linear part of the curve, after which there is a drop in the micropump performance. The excitation laser diode has a power consumption that is independent to the micropump’s performance, so the linear section of the process yields maximum efficiency.

We observe that the linear flow rate appears to be relatively constant among compositions 2, 3 and 4 at about  $2.22 \mu\text{l/s}$  and comparably repeatable (Table 1, Row 6), bearing in mind the error margin defined by the setup itself. Series 1, having the lowest content in microspheres and absorbance agent, has a lower linear flow rate. By increasing the content in microspheres and absorbance agent, the duration of the linear section (Table 1, Row 5), the linear volume displaced (Table 1, Row 7) and the total volume displaced (Table 1, Row 8) all increase.

Examining the dependence of the linear flow rate from the concentration of the absorbance agent separately (Fig. 2C), we

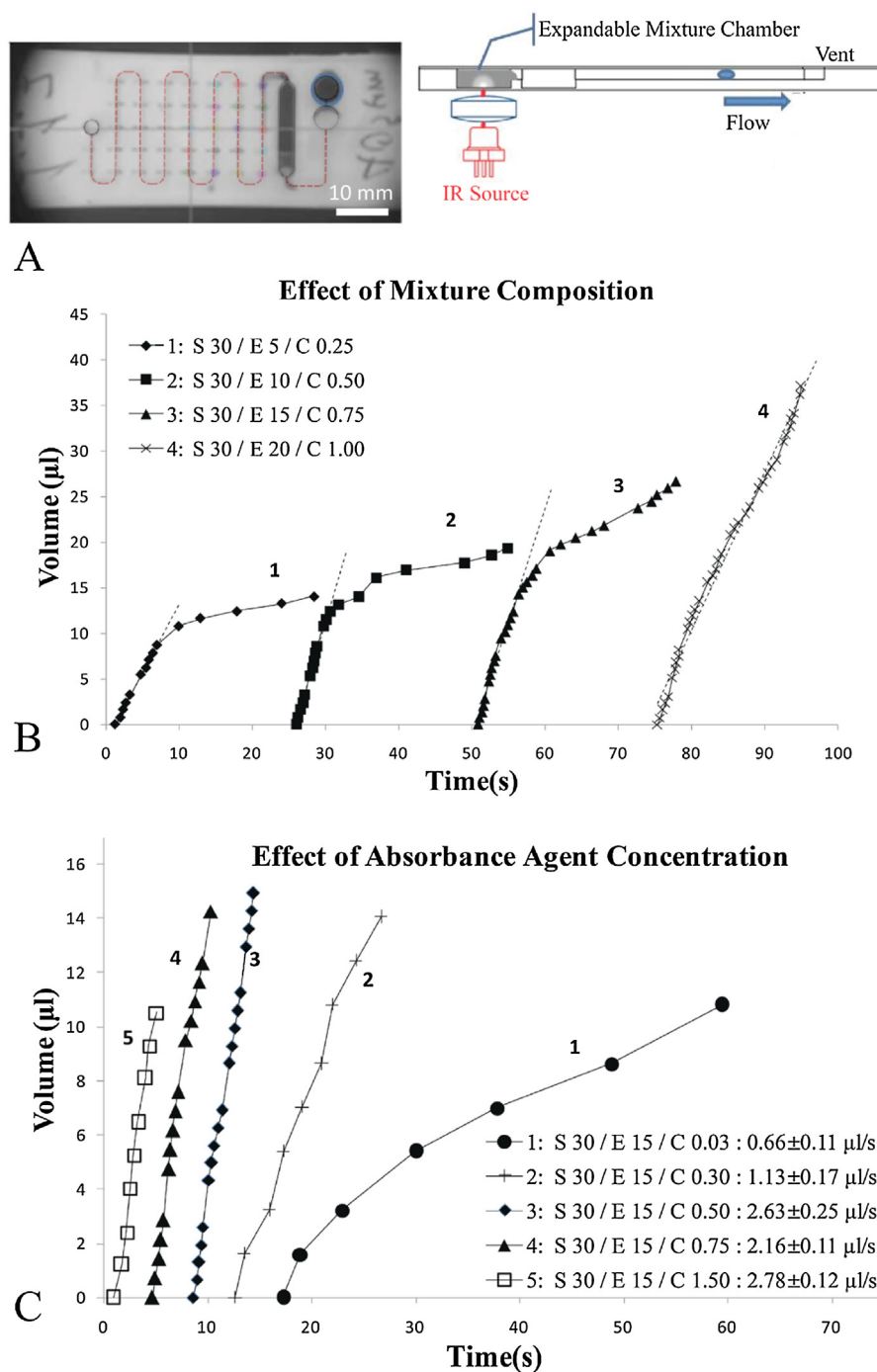


**Fig. 2.** Micropump performance in correlation to the mixture composition. Presentation of sample curves. (A) The microfluidic chip used in the experiments, (B) volume displacement for different expanding microspheres (marked: E) and absorbance agent concentrations (marked: C) in w/w (mass units) of dimethicone (marked: S) as seen in the legends of the diagrams, (C) volume displacement for different absorbance agent concentrations in fixed expanding microsphere content.

observe that for low concentrations, a rise in the agent content leads to a rise in the  $\mu\text{l/s}$  that can be achieved. However, there is a threshold after which an increase in the said content will not significantly affect the flow rate. In particular, the two lowest concentrations in absorbance agent yield an average of  $0.66$  and  $1.13 \mu\text{l/s}$ , respectively, while the three consequent concentrations display  $2.63$ ,  $2.16$  and  $2.78 \mu\text{l/s}$ , respectively. While moving from the lower to the higher concentrations of the absorbance agent we see an evident trend to increase the absorbed energy, there is a limit to how much energy can be absorbed given the current setup.

### 3.3. Precise volume displacement

The proposed micropumping method so far utilizes an open loop control scheme to obtain a median value for each variable of interest within an error range. A limitation of this approach is that precise volume displacement is not possible. In order to overcome this, we developed a method of volume control in which a UV photopolymer is placed in line with the micropump so as to move along with the fluid reagent. In a predefined distance along the microfluidic channel, a  $405 \text{ nm}$  laser diode has been placed and is switched on along with the IR laser that causes the mixture to expand. When

**Table 1**

Micropumping characteristics vs. mixture composition. The error is represented by the standard deviation encountered during these experiments. Each experiment was conducted 5 times.

|                          |                                | Mixture Composition |                |                |                 |
|--------------------------|--------------------------------|---------------------|----------------|----------------|-----------------|
| Experiment series        |                                | 1                   | 2              | 3              | 4               |
| Dimethicone Content      |                                | 30                  | 30             | 30             | 30              |
| Expancel® Content        |                                | 5                   | 10             | 15             | 20              |
| Absorbance Agent Content |                                | 0.25                | 0.50           | 0.75           | 1.00            |
| Flow Characteristics     | Duration of Linear section (s) | 6.12<br>±1.44       | 6.97<br>±1.83  | 9.69<br>±3.40  | 16.47<br>±4.46  |
|                          | Linear Flow Rate (μl/sec)      | 1.54<br>±0.04       | 2.29<br>±0.41  | 2.16<br>±0.25  | 2.22<br>±0.61   |
|                          | Linear Volume Displaced (μl)   | 8.39<br>±1.67       | 14.51<br>±1.82 | 19.37<br>±5.27 | 36.89<br>±3.87  |
|                          | Total Volume Displaced (μl)    | 18.46<br>±4.04      | 37.36<br>±2.19 | 74.78<br>±2.62 | 161.54<br>±3.53 |

the photopolymer reaches the path of the laser beam, it rapidly increases its viscosity and eventually solidifies, thus isolating the pressurized part of the channel from the rest (Fig. 3A). This is done in attempt to define how much reagent is going to be pumped and also to cancel out the retraction feature of this method that has been mentioned in Section 3.1. The chip design consists of  $2 \times 40 \mu\text{l}$  chambers connected in line for the expandable mixture and the photopolymer, respectively. A microfluidic channel of  $500 \mu\text{m}$  depth and 1 mm width is placed after the photopolymer chamber. In a user specified distance along the channel, there is a flat end circular pocket acting as an optical window for the N-UV laser beam. The experimental procedure requires the activation of the expandable mixture by turning the IR laser diode on, while at the same time the N-UV diode is also activated. The expansion causes the photopolymer and the liquid reagent both to move forward in line until the photopolymer reaches the N-UV laser beam, at which point it solidifies and stops all flow in the circuit.

The expandable mixture utilized in these experiments was a 30/15/1.5 w/w composition of Dimethicone, Expancel® DU 40 particles and carbon black powder. We conducted six repetitions under the same experimental conditions in order to assess the repeatability of this method. Fig. 3B shows a significantly lowered flow rate compared to the experiments conducted in Section 3.2, due to the viscosity of the photopolymer utilized in this method. Nevertheless, the total displaced volume in all experiments falls within a  $0.7 \mu\text{l}$  zone, having an average displaced volume equal to  $5.94 \pm 0.11 \mu\text{l}$  ( $\pm 1$  standard error). It should be noted that the deviation from a nominal value in this experiment shows no correlation with the displaced volume quantity, but depends on the optical design and fabrication of the laser beam window, mainly because of scattering that affects the photopolymer before it reaches the polymerization spot. It should be noted that the results obtained from this experiment display higher deviations than the ones encountered in our previous experiments. A different experimental setup that was used here allows for expanded microspheres to move through the port connecting the mixture filled chamber and the empty chamber. This is a source of error that decreases traveling mixture homogeneity and consequently affects flow rate repeatability.

### 3.4. Pressure testing

In order to assess the functionality of the micropump when elevated pressure is encountered (i.e. when using viscous fluids or lengthy channels), a similar design to the one described in Section 3.2 was used. However this time instead of venting the outlet, it was connected to a pressure generator (Fig. 4A). The experimental procedure of Section 3.2 was repeated using one composition of the expanding mixture (dimethicone: 30/expandable microspheres: 15/carbon black: 1.5 w/w) under back pressures ranging from 0 to 150 mbar relative to atmospheric. The micromachined chip embeds two chambers to facilitate the storage and expansion of the mixture, one chamber for the fluid reagent storage and a semi-circular profile channel of  $500 \mu\text{m}$  radius for the displacement and tracking of the latter. The laser source was adjusted to output approximately half the power that was used in the previous experiments (531 mW reduced to 265 mW).

Fig. 4B shows no evident trend linking outlet pressures of this magnitude with the flow rate, however repeatability errors like the ones seen in Section 3.3 are also present here. We believe that the apparent indifference of the pump performance toward the outlet pressure is due to the fact that the actual pressure needed to push the expandable mixture through channels is much higher than the 150 mbar that we apply on the outlet. This is to be expected if we consider that the expandable mixture is highly viscous ( $\sim 10^5$  cP) and thus in need of high pressures to move across microfluidic chambers. The theoretical maximum pressure that can be countered by the proposed technology is the vapor pressure of the encapsulated hydrocarbon within the beads. This has been reported to be 16.2 bar at  $90^\circ\text{C}$  [21] for the microspheres being used in this experiment. In a separate set of experiments that we conducted, the same expandable mixture was activated within chips that were fully sealed. The initial air volume was compared to the minimum (pressurized) air volume observed during five identical experiments to obtain a maximum generated pressure equal to 9.2 bar using the van der Waals equation.

### 3.5. Thermal imaging

An important consideration when designing a thermal micropump is the heat transfer from the pump to the reagents in nearby positions. As described in Section 3.1, we employ layer-by-layer activation of the mixture through localized heating. In order to assess heat transfer during the expansion process, we repeated the experiment in Section 3.2 using a calibrated thermal imaging camera to quantify chip temperature (Fig. 5).

Fig. 5 shows the temperature distribution just before the beam exits the mixture chamber, which is the peak temperature point during of the expansion process. We notice that the chamber and channels are near the temperature threshold boundary but remain under  $37^\circ\text{C}$ . The highest recorded temperature was  $92.3^\circ\text{C}$  at the center of the chamber. The lowest temperature was  $26.1^\circ\text{C}$ , the chip body temperature, which was cooled to  $20^\circ\text{C}$  prior to the experiment in order to be distinguishable from the environment in thermal images. It should be noted that the ambient temperature during the experiment was  $31^\circ\text{C}$  and that the test platform below the chip was a flat machined aluminum plate which does contribute to the heat transfer of the process through heat conduction from the chip to the environment. These results are significant because excessive heat could cause biological assays to suffer from denaturation and other temperature related processes. Additionally, they serve as an indication that the expansion is not due to liquid reagent evaporation or air expansion, but due to microsphere expansion and rupture.

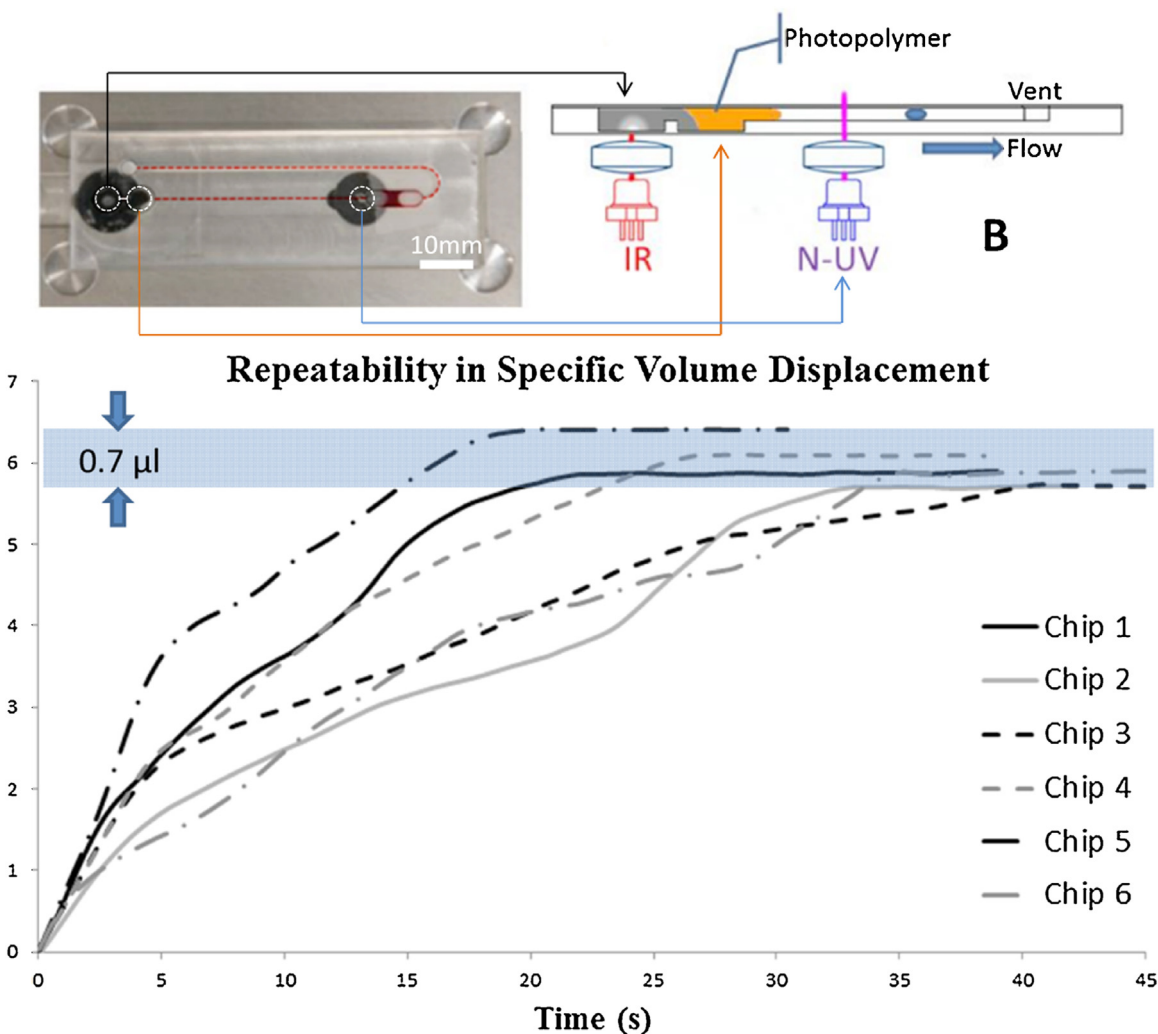


Fig. 3. Experiments for the assessment of a method for predefined volume displacement. (A) The microfluidic chip design used for these experiments, (B) The volume displacement profiles of each repetition of the experiment, all concluding within a 0.7 µl wide zone around a nominal value after the solidification of the photopolymer.

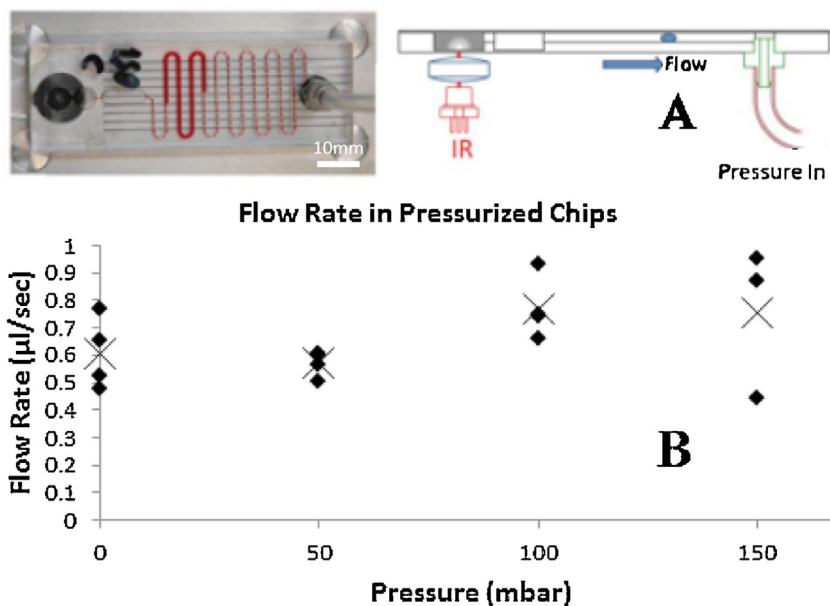
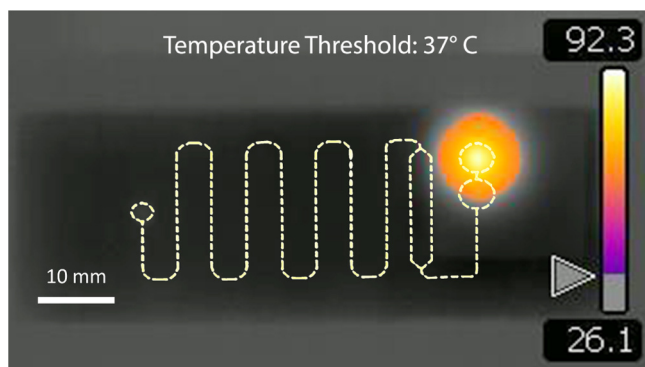


Fig. 4. Flow rate in pressurized microfluidic channels. (A) The microfluidic chip design used for these experiments (B) flow rates for the linear part of the expansion working against outlet pressure. (X) marks the mean values



**Fig. 5.** Thermal imaging at the peak temperature with 37 °C threshold below which areas are presented in grayscale. Chip structure has been added in dashed lines for better representation.

#### 4. Discussion and future work

We have demonstrated a prototype version of a single use micropumping system that requires only one laser source to achieve volume displacement. It has been shown that volumes over 35  $\mu\text{l}$  can be easily displaced within a few seconds with an approximately constant flow rate. The volume displacement has been shown to occur in two phases, a linear and a non-linear, out of which the first one yields maximum energy efficiency. The flow rate depends on the concentration of absorbance agent in the mixture, while the maximum volume that can be displaced depends on both the concentration of expandable microspheres and the volume of available mixture that is found along the laser beam path. We have shown that repeatability of less than 1  $\mu\text{l}$  is possible by using a 405 nm laser source and a photopolymer, as a volume dependent shutoff valve. Additionally, it has been demonstrated that pressures up to 150 mbar will not affect the micropump's performance and that the heat transfer implications of the method can be contained so as not to affect active reagents on the chip. Finally, while it has not been investigated in depth, we have observed that after the expansion process, a recovery phase occurs. This phase could be used to enable liquid reagent aspiration from the environment to the chip.

This method is limited by the deviation of the measured flow rates and displaced volumes. This, we believe, is due to the dimensional deviations of the chips and the sensitivity of the method to the repeatability of the experimental conditions in respect to laser optics, i.e. beam power stability, focal point and transmittance of optical windows. Thus, optimization of these parameters is a necessary step for the improvement of repeatability. Another limitation is the energy consumption of this method ( $\sim 1.5 \text{ J}/\mu\text{l}$  moved) that is related to the efficiency of the laser sources and is also in need of optimization.

Possible applications of the proposed method are numerous in the fields of biology, medicine, point of care diagnostics and environmental research. Compared to the state of the art for fluid handling in microfluidics, the main advantages are four: (1) We identify the potential for a unified optofluidic technology in which fluid handling and detection are both done using only laser diodes or even just one laser diode. (2) The micropumping technology is embedded as a single use feature in the disposable microfluidic chips, thus removing the need for peripheral fluid handling hardware. (3) There is no need for tubing and tubing connectors, frequent sources of problems in microfluidic systems. (4) Even though it is not in an optimized state, this technology appears to already provide adequate performance for most applications at a small fraction of the cost.

The method can be easily scaled up by integrating multiple chambers, each performing a single task. In that way, multistep protocols such as ELISA assays can be realized in microfluidic chips powered by a single pocket-size device that need only contain a PCB assembly with embedded laser diodes and a camera or even a smartphone adapter. For more demanding applications that would make dedicated laser diodes an uneconomical solution, a device very closely modeled to a Blu-ray burner with appropriate firmware could also be used, since such devices often embed high power 405 nm laser diodes that could be used both for activation of the expandable mixture and the photopolymer as well as for fluorescent marker excitation. In this case the microfluidic chip could be modeled to resemble the compact disk designs or simply fit in a CD shaped adapter. Such a solution would benefit from the Lab on a CD technology that has already been developed. The microfluidic chips themselves can be produced using simple molding techniques, since single layer structures suffice for this fluid handling method, thus making this technology advantageous for mass production.

The proposed method is currently under evaluation as a tool for valving and aspiration. Subsequently an effort to optimize the process and reduce deviations in respect to flow rate and displacement precision and repeatability will be made. Should these steps provide with equally promising results, we believe that the fabrication of reliable no-moving-part PoC devices and single-diode high-throughput platforms for multistep assay preparation and detection will be possible.

#### Acknowledgments

We would like to thank Professor M. Kandyla for helping us with the laser power measurements. We are also grateful to D. Tzeranis, T. Sakellaropoulos, N. Georgiou and the NTUA Systems Bioengineering group for their comments and guidance throughout the writing of this paper. We thank AkzoNobel for providing us with the Expancel<sup>®</sup> microspheres.

This work was supported by the European Union (European Social Fund – ESF) – Greek national funds through the Operational Program “Education and Lifelong Learning” of the National Strategic Reference Framework (NSRF) – Research Funding Program ERC “Investing in knowledge society through the European Social Fund” (Grant no. ERC-11/MIS:374071).

#### Appendix A. Supplementary data

Supplementary data associated with this article can be found, in the online version, at <http://dx.doi.org/10.1016/j.snb.2015.04.101>

#### References

- [1] A.K. Au, H.Y. Lai, B.R. Utela, A. Folch, Microvalves and micropumps for BioMEMS, *Micromachines-Basel* 2 (2011) 179–220.
- [2] M.A. Unger, H.P. Chou, T. Thorsen, A. Scherer, S.R. Quake, Monolithic microfabricated valves and pumps by multilayer soft lithography, *Science* 288 (2000) 113–116.
- [3] O.C. Jeong, S. Konishi, Fabrication of a peristaltic micro pump with novel cascaded actuators, *J. Micromech. Microeng.* 18 (2008).
- [4] W.H. Grover, A.M. Skelley, C.N. Liu, E.T. Lagally, R.A. Mathies, Monolithic membrane valves and diaphragm pumps for practical large-scale integration into glass microfluidic devices, *Sens. Actuators B: Chem.* 89 (2003) 315–323.
- [5] H. Lai, A. Folch, Design and dynamic characterization of single-stroke peristaltic PDMS micropumps, *Lab Chip* 11 (2011) 336–342.
- [6] J. Kim, J. Baek, K. Lee, Y. Park, K. Sun, T. Lee, et al., Photopolymerized check valve and its integration into a pneumatic pumping system for biocompatible sample delivery, *Lab Chip* 6 (2006) 1091–1094.
- [7] M.C. Tracey, I.D. Johnston, J.B. Davis, C.K.L. Tan, Dual independent displacement-amplified micropumps with a single actuator, *J. Micromech. Microeng.* 16 (2006) 1444–1452.
- [8] S.S. Wang, X.Y. Huang, C. Yang, Valveless micropump with acoustically featured pumping chamber, *Microfluid Nanofluid* 8 (2010) 549–555.
- [9] W. Gu, X.Y. Zhu, N. Futai, B.S. Cho, S. Takayama, Computerized microfluidic cell culture using elastomeric channels and Braille displays, *Proc. Natl. Acad. Sci. U.S.A.* 101 (2004) 15861–15866.

- [10] S. Bohm, W. Olthuis, P. Bergveld, An integrated micromachined electrochemical pump and dosing system, *Biomed. Microdevices* 1 (1999) 121–130.
- [11] C.H. Chen, J.G. Santiago, A planar electroosmotic micropump, *J. Microelectromech. Syst.* 11 (2002) 672–683.
- [12] A.R. Tovar, A.P. Lee, Lateral cavity acoustic transducer, *Lab Chip* 9 (2009) 41–43.
- [13] A.V. Lemoff, A.P. Lee, An AC magnetohydrodynamic micropump, *Sens. Actuators B: Chem.* 63 (2000) 178–185.
- [14] M.G. Pollack, R.B. Fair, A.D. Shenderov, Electrowetting-based actuation of liquid droplets for microfluidic applications, *Appl. Phys. Lett.* 77 (2000) 1725–1726.
- [15] K. Hosokawa, K. Sato, N. Ichikawa, M. Maeda, Power-free poly(dimethylsiloxane) microfluidic devices for gold nanoparticle-based DNA analysis, *Lab Chip* 4 (2004) 181–185.
- [16] D.B. Franz Weinert, Light Driven Microfluidics, *Optomechatronic Technologies*, IEEE, Istanbul, 2009.
- [17] M. Takeuchi, M. Hagiwara, G. Haulot, C.M. Ho, Reconfigurable microfluidic pump enabled by opto-electrical-thermal transduction, *Appl. Phys. Lett.* 103 (2013).
- [18] P. Griss, H. Andersson, G. Stemme, Expandable microspheres for the handling of liquids, *Lab Chip* 2 (2002) 117–120.
- [19] N. Roxhed, S. Rydholm, B. Samel, W. van der Wijngaart, P. Griss, G. Stemme, A compact, low-cost microliter-range liquid dispenser based on expandable microspheres, *J. Micromech. Microeng.* 16 (2006) 2740–2746.
- [20] S. Spieth, A. Schumacher, C. Kallenbach, S. Messner, R. Zengerle, The NeuroMedicator—a micropump integrated with silicon microprobes for drug delivery in neural research, *J. Micromech. Microeng.* 22 (2012).
- [21] M. Lynda, Fluid Manipulation Using a Thermoexpandable Polymer Based on Polydimethylsiloxane and Expancel [PhD], Ecole Polytechnique Federal De Lausanne, 2010.

## Biographies

**G.P. Kanakaris** is a Mechanical Engineer specializing in mechanical design and biotechnology instrument development. He has acquired his M.Sc. from the National Technical University of Athens, 2011. His research interests include high throughput proteomic measurement platforms as well as Point of Care Systems for in vitro diagnostics. He is currently a PhD candidate in the field of proteomic measurement technologies.

**N. Fatsis-Kavalopoulos** is a Mechanical Engineer specializing in mechanical design and BioEngineering. He is a graduate of the National Technical University of Athens, School of Mechanical Engineering. His work focuses on the design and fabrication of BioMEMS and  $\mu$ TAS, aiming at the automation and optimization of biochemical and biological assays and the development of embedded systems, aiming at advancements in diagnostics and disease prevention.

**L.C. Alexopoulos** is an assistant professor in the Dept. of Mechanical Engineering at NTUA and director of the Systems Bioengineering group. He studied at Aristotle University of Athens (Mech. Eng. Dipl. 1998), Duke (PhD, Dept. of Biomedical Eng. in 2004), MIT (PostDoc, Dept. of Biological Eng. 2004–2008), and Harvard Medical School (PostDoc, Dept. of Systems Biology 2006–2008). He is currently the principal investigator in a multidisciplinary team comprising engineers (mechanical, electrical and chemical disciplines), computer scientists, biologists and medical doctors working in the area of Systems Biology and Medical Devices. The Systems Bioengineering group integrates novel biological and engineering approaches with emphasis on modeling biological systems,  $\mu$ TAS, multiplex technology, and proteomic profiling.